

AN EFFICIENT SAI PRECONDITIONING TECHNIQUE FOR HIGHER ORDER HIERARCHICAL MLFMM IMPLEMENTATION

D. Z. Ding, R. S. Chen, and Z. H. Fan

Department of Communication Engineering
Nanjing University of Science and Technology
Nanjing 210094, China

Abstract—A new set of higher order hierarchical basis functions based on curvilinear triangular patch is proposed for expansion of the current in electrical field integral equations (EFIE) solved by method of moments (MoM). The multilevel fast multipole method (MLFMM) is used to accelerate matrix-vector product. An improved sparse approximate inverse (SAI) preconditioner in the higher order hierarchical MLFMM context is constructed based on the near-field matrix of the EFIE. The quality of the SAI preconditioner can be greatly improved by use of information from higher order hierarchical MLFMM implementation. Numerical experiments with a few electromagnetic scattering problems for open structures are given to show the validity and efficiency of the proposed SAI preconditioner.

1. INTRODUCTION

Electromagnetic integral equations are often discretized with the method of moments (MoM) [1–7], one of the most widespread and generally accepted techniques for electromagnetic problems. The formulation considered in this paper is the electric field integral equation (EFIE) as it is the most general and does not require any assumption about the geometry of the object. It is convenient to model objects with arbitrary shape using triangular patches; hence, RWG functions [8] are widely used for representing unknown current distributions. When iterative solvers are used to solve the MoM matrix equation, the fast multipole method (FMM) or multilevel fast multipole method (MLFMM) [9–15] can be used to accelerate the calculation of matrix-vector multiplies. However, the RWG functions have a poor convergence and need a large number of unknowns for

a desired accuracy. To circumvent this disadvantage, a remedy is to employ higher order basis functions.

In this paper, a new set of higher order hierarchical basis functions [16, 17] based on curvilinear triangular patch is constructed in MoM, which is derived from the TVFE's for finite element method (FEM) discretization proposed by Andersen and Volakis [16]. The new proposed basis set is convenient to model objects with arbitrary shape using curve triangular patches compared with the hierarchical Legendre basis functions for a quadrilaterals element proposed by Jorgensen et al. in [17]. Hierarchical functions allow for much greater flexibility. The basis of order M is a subset of the basis of order $M + 1$, which allows mixing of different order bases in the same mesh. Thus, hierarchical bases combine the advantages of both low-order and higher order bases into a single flexible basis. This desirable property allows for selective field expansion using different order bases in different regions of the computational domain. Lowest order bases can be employed in regions where the field is expected to vary slowly whereas higher order bases can be employed in regions where rapid field variation is anticipated.

The system matrix resulted from EFIE with the higher order hierarchical basis functions is often an ill-conditioned matrix and results in the low convergence of the Krylov iterative method [18]. Simple preconditioners like the diagonal or diagonal blocks of the coefficient matrix can be effective only when the matrix has some degree of diagonal dominance [19]. Incomplete LU (ILU) preconditioners have been successfully used on nonsymmetric dense systems in [20], but the factors of the ILU preconditioner may become very ill-conditioned and consequently the performance is very poor [21]. As an attempt for a possible remedy, the new perturbed ILU preconditioner is proposed [22]. The key idea is to perturb the near-field impedance matrix of EFIE with the principle value term of the magnetic field integral equation (MFIE) operator before constructing ILU preconditioners. The perturbed ILU preconditioner is just applied for electromagnetic scattering problems of closed objects in [22]. An effective sparse approximate inverse (SAI) preconditioner suitable for implementation in the FMM context has also been proposed [23], which is based on a Frobenius-norm minimization with a priori sparsity pattern selection strategy. The performance of SAI preconditioner is greatly influenced by the way of choosing nonzero pattern and the way of solving the least-squares problems in the minimization process. In this paper, information from higher order hierarchical MLFMM implementation is employed to develop a high quality SAI preconditioner, resulting in a faster convergence rate [24].

This paper is outlined as follows. Section 2 gives an introduction of EFIE formulation combined with the higher order hierarchical basis function. Section 3 describes the details to construct the SAI preconditioner by use of information from higher order hierarchical MLFMM implementation based on the near-field matrix. Numerical examples are given to demonstrate the accuracy and efficiency of the proposed method in radar cross section (RCS) calculations in Section 4. Section 5 gives some conclusions and comments.

2. HIGH ORDER HIERARCHICAL BASIS FUNCTION

Consider an arbitrarily-shaped 3-D conducting object illuminated by an incident field \mathbf{E}^i , the EFIE is given by (an $e^{-i\omega t}$ time convention has been assumed and suppressed)

$$-\frac{k\eta i}{4\pi} \hat{t} \cdot \int_S \bar{\mathbf{G}}(\mathbf{r}, \mathbf{r}') \cdot \mathbf{J}(\mathbf{r}') dS' = \hat{t} \cdot \mathbf{E}^i(\mathbf{r}) \quad (1)$$

where k is wavenumber, η is impedance, \hat{t} is the unit tangential vector, \mathbf{r}' and \mathbf{r} are source point and observation point on S , respectively. $\mathbf{J}(\mathbf{r})$ denotes the unknown surface current density, and $\bar{\mathbf{G}}(\mathbf{r}, \mathbf{r}')$ is defined by

$$\bar{\mathbf{G}}(\mathbf{r}, \mathbf{r}') = \left[\bar{\mathbf{I}} - \frac{1}{k^2} \nabla \nabla' \right] \frac{e^{ik|\mathbf{r}-\mathbf{r}'|}}{|\mathbf{r}-\mathbf{r}'|} \quad (2)$$

The EFIE can be solved by MoM. The conducting surface is subdivided into small triangular patches and the unknown current $\mathbf{J}(\mathbf{r})$ is first expanded as

$$\mathbf{J}(\mathbf{r}) = \sum_{i=1}^N \mathbf{I}_i \mathbf{f}_i(\mathbf{r}) \quad (3)$$

where N is the number of unknowns, $\mathbf{f}_i(\mathbf{r})$ denote the vector basis functions and \mathbf{I}_i is the unknown expansion coefficients. Applying Galerkin's method results in a matrix equation

$$\sum_{n=1}^N A_{mn} I_n = b_m, \quad m = 1, 2, \dots, N \quad (4)$$

where

$$A_{mn} = \frac{-k\eta i}{4\pi} \int_s \mathbf{f}_m(\mathbf{r}) \cdot \int_{s'} \bar{\mathbf{G}}(\mathbf{r}, \mathbf{r}') \cdot \mathbf{f}_n(\mathbf{r}') ds ds' \quad (5)$$

$$b_m = \int_s \mathbf{f}_m(\mathbf{r}) \cdot \mathbf{E}^i(\mathbf{r}) ds \quad (6)$$

The factor that most limits the capability of the MoM is the number of unknowns. As pointed out in the introduction, this limitation can be relaxed by using higher order basis functions. For a given accuracy, the use of higher order basis functions allows us to use larger triangular patches to discrete the objects. A new set of higher order hierarchical basis functions is developed for MoM. The proposed class of hierarchical basis function is based on the hierarchical TVFE's introduced in [16].

Divergence-conforming bases \bar{f}_β^e on 2-D elements can be obtained by forming the cross product of the associated curl-conforming bases \bar{W}_β^e with the unit vector \hat{n} normal to the element [25] and defined as follows:

$$\bar{f}_\beta^e = \bar{W}_\beta^e \times \hat{n} \quad (7)$$

Thus, the divergence-conforming bases of order 0.5 on the above Lars S. Andersen's curl-conforming basis functions are

$$\bar{f}_1^e = (\xi_2 \nabla \xi_3 - \xi_3 \nabla \xi_2) \times \hat{n} \quad (8)$$

$$\bar{f}_2^e = (\xi_3 \nabla \xi_1 - \xi_1 \nabla \xi_3) \times \hat{n} \quad (9)$$

$$\bar{f}_3^e = (\xi_1 \nabla \xi_2 - \xi_2 \nabla \xi_1) \times \hat{n} \quad (10)$$

with

$$\nabla \xi_2 = \frac{\hat{n} \times \bar{I}_1}{J}, \quad \nabla \xi_3 = \frac{\hat{n} \times (\bar{I}_2 - \bar{I}_1)}{J} \quad (11)$$

where J is the Jacobian, ξ_1, ξ_2, ξ_3 are the simplex coordinates, \bar{I}_i ($i = 1, 2, 3$) represents the edge vector opposite to the nodes 1, 2, and 3, respectively. The divergence-conforming bases of order 0.5 based on curvilinear triangular patch are shown in Figure 1. Taking (11) into (8)–(10), we obtain the divergence-conforming bases of order 0.5

$$\bar{f}_1^e = \frac{1}{J} (\xi_2 \bar{I}_3 - \xi_3 \bar{I}_2) \quad (12)$$

$$\bar{f}_2^e = \frac{1}{J} (\xi_3 \bar{I}_1 - \xi_1 \bar{I}_3) \quad (13)$$

$$\bar{f}_3^e = \frac{1}{J} (\xi_1 \bar{I}_2 - \xi_2 \bar{I}_1) \quad (14)$$

As described in the above, the hierarchical basis functions of order 1.5 can be obtained by forming the cross product of the curl-conforming bases \bar{W}_β^e with the unit vector \hat{n} and defined as

$$\bar{f}_1^e = \frac{1}{J} (\xi_2 \bar{I}_3 - \xi_3 \bar{I}_2) \quad (15)$$

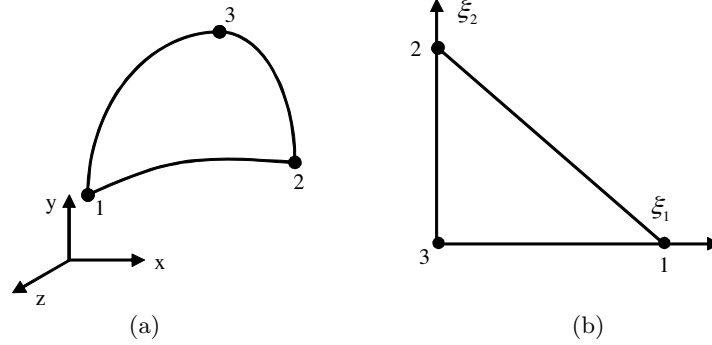


Figure 1. Example of divergence-conforming bases of order 0.5 based on curvilinear triangular patch: (a) a cell of curvilinear triangular patch in the xyz coordinate system, (b) the projection of the curvilinear triangular patch in the simplex coordinate system.

$$\bar{f}_2^e = \frac{1}{J} (\xi_3 \bar{I}_1 - \xi_1 \bar{I}_3) \quad (16)$$

$$\bar{f}_3^e = \frac{1}{J} (\xi_1 \bar{I}_2 - \xi_2 \bar{I}_1) \quad (17)$$

$$\bar{f}_4^e = \frac{1}{J} (\xi_2 - \xi_3) (\xi_2 \bar{I}_3 - \xi_3 \bar{I}_2) \quad (18)$$

$$\bar{f}_5^e = \frac{1}{J} (\xi_3 - \xi_1) (\xi_3 \bar{I}_1 - \xi_1 \bar{I}_3) \quad (19)$$

$$\bar{f}_6^e = \frac{1}{J} (\xi_1 - \xi_2) (\xi_1 \bar{I}_2 - \xi_2 \bar{I}_1) \quad (20)$$

$$\bar{f}_7^e = \frac{1}{J} \xi_1 (\xi_2 \bar{I}_3 - \xi_3 \bar{I}_2) \quad (21)$$

$$\bar{f}_8^e = \frac{1}{J} \xi_2 (\xi_3 \bar{I}_1 - \xi_1 \bar{I}_3) \quad (22)$$

The hierarchical basis functions are ideally suited for employing an efficient selective field expansion where different order basis functions are employed in different regions of the computational domain. Hence, for a uniform mesh, the lowest order basis functions can be employed in regions where the field is expected to experience smooth variation (regions where the relative material parameters are (nearly) unity, away from edges, etc.) whereas a higher order basis functions can be employed in regions where the field is expected to vary rapidly (near edges close to material boundaries, in dense materials. etc.).

A generalization of the hierarchical basis functions of order 2.5 and even higher order ones can be obtained in a similar way. Finally, the

element of the impedance matrix A_{mn} is evaluated with the presented hierarchical basis functions. The linear system of equations in (4) can be solved by the restart GMRES iterative method using MLFMM to accelerate the matrix-vector multiplication. Note that in MLFMM, A_{mn} is evaluated only when f_m and f_n are inside the same or nearby groups.

3. THE IMPROVED SAI PRECONDITIONER

It is well known that the convergence rate of an iterative solution is dependent upon the spectral radius of the matrix equation system. The use of higher order hierarchical basis functions increases the condition number of the system. In order to speed up the convergence rate of Krylov methods, preconditioning techniques are employed to transform the EFIE matrix equations into an equivalent form

$$\mathbf{M}_h \mathbf{A}_h \mathbf{x} = \mathbf{M}_h \mathbf{b} \quad (23)$$

where \mathbf{A}_h is the EFIE impedance matrix associated with the higher order hierarchical basis functions and \mathbf{M}_h is the corresponding preconditioner. The purpose of preconditioning is to make the preconditioned matrix $\mathbf{M}_h \mathbf{A}_h$ better conditioned than the original matrix \mathbf{A}_h .

A SAI preconditioner is considered based on a Frobenius-norm minimization procedure. SAI computes a SAI for the coefficient matrix A as the matrix $M_h = \{m_{ij}\}$, which minimizes $\|\mathbf{I} - \mathbf{M}_h \mathbf{A}_h\|_F$ subject to certain sparsity constraints. Owing to the rapid decay of the discrete Green's function, most of large entries in the impedance matrix \mathbf{A}_h are located in its near-part matrix \mathbf{A}_{hn} . \mathbf{A}_{hn} is the symmetric near-field matrix of the EFIE impedance matrix \mathbf{A}_h associated with the higher order hierarchical basis functions. Therefore, in the MLFMM context, the near-part matrix \mathbf{A}_{hn} is widely used as the basis for constructing preconditioners. The Frobenius-norm is usually chosen because it allows the decoupling of the constrained minimization problem into N independent linear least-squares problems for each row of M_h (when preconditioning from the left).

$$\|\mathbf{I} - \mathbf{M}_h \mathbf{A}_{hn}\|_F^2 = \|\mathbf{I} - \mathbf{M}_h \mathbf{A}_{hn}^T\|_F^2 = \sum_{j=1}^N \|e_j - A_{hn} m_j\|_2^2 \quad (24)$$

where e_j is the j -th unit vector and m_j is the column vector representing the j -th row of M_h . The main issue for the computation of SAI preconditioner is the selection of the nonzero pattern for M_h ,

that is, the set of indices

$$S = \{(i, j) \in [1, N]^2 \mid s \cdot t \cdot m_{ij} \neq 0\}$$

If the sparsity of M_h is known, the nonzero structure for the j -th column of M_h is automatically determined and defined as

$$J = \{i \in [1, N] \mid s \cdot t \cdot i, j \neq 0\}$$

Then, the solution of the least-squares problems (24) involves only the columns of \mathbf{A}_{hn} indexed by J , which can be denoted by $\mathbf{A}_{hn}(:, J)$. Because \mathbf{A}_{hn} is sparse, many rows in $\mathbf{A}_{hn}(:, J)$ are usually null, not affecting the solution of the least-squares problems. I is the set of indices corresponding to the nonzero rows in $\mathbf{A}_{hn}(:, J)$. We defined $\hat{\mathbf{A}}_{hn} = \mathbf{A}_{hn}(I, J)$ as the “reduced” form corresponding to the nonzero pattern for M_h . And then we defined the column vector of M_h corresponding to the nonzero rows in $\mathbf{A}_{hn}(:, J)$ by $\hat{\mathbf{m}}_j = m_j(\mathbf{J})$, and the j -th unit vector corresponding to the nonzero rows in $\mathbf{A}_{hn}(:, J)$ by $\hat{\mathbf{e}}_j = e_j(\mathbf{J})$. Thus, the least-squares problems can be transformed into the “reduced” form

$$\min \left\| \hat{\mathbf{e}}_j - \hat{\mathbf{A}}_{hn} \hat{\mathbf{m}}_j \right\|_2^2, \quad j = 1, \dots, N \quad (25)$$

Usually the “reduced” least-squares problems (25) have much smaller size than that of least-squares problems (24). In MLFMM, N higher order hierarchical basis functions are divided into R groups, denoted by G_p ($p = 1, 2, \dots, R$). Make a close look at the higher order hierarchical MLFMM implementation, we can find that each higher order hierarchical basis function in one group on the finest level couples with the higher order basis functions in the same and the adjacent groups on the same level via the near-field matrix. Therefore, each basis function in a group couples with the same set of higher order basis functions in the near-field matrix. Based on this information, we can now further reduce the size of the least-squares problems defined by formulation (25).

Let j -th group be denoted by G_j and its neighbors by NG_j (not including itself), then the nonzero structure for all columns of M_h corresponding to the hierarchical basis functions in the group G_j can be determined and defined as:

$$J = \{i \in [1, N] \mid s \cdot t \cdot i \in G_j \text{ or } i \in NG_j\}$$

Suppose NNG_j to be neighbor groups of NG_j (also not including itself), the nonzero structure of the above defined submatrix $\mathbf{A}_{hn}(:, J)$, is constrained by the set of indices I defined as:

$$I = \{i \in [1, N] \mid s \cdot t \cdot i \in G_j \text{ or } i \in NG_j \text{ or } i \in NNG_j\}$$

We defined the newly constrained near-field matrix by $\bar{\mathbf{A}}_{hn}$. And then we defined the j -th column vector of M_h and unit vector corresponding to the nonzero rows in the newly constrained near-field matrix $\bar{\mathbf{A}}_{hn}$ by \bar{M}_j and \bar{E}_j , respectively. Thus, the least-squares problems can be further reduced into the form of

$$\min \|\bar{\mathbf{E}}_j - \bar{\mathbf{A}}\bar{M}_j\|_2^2, \quad j = 1, \dots, M \quad (26)$$

where R is the number of groups on the finest level in MLFMM. Since R is usually much smaller than N , the construction cost of the SAI preconditioner can be significantly cut down by using formulation (26) instead of (25).

To capture stronger couplings between the basis functions and to keep the size of the problems (26) to be smaller, we apply two filtrations to the set of indices J and I , respectively, as follows:

$$J = \{i \in [1, N] (i \in G_j \text{ or } i \in NG_j) \text{ and } (\text{dist}(i, j) \leq \tau_1)\} \quad (27)$$

$$I = \{i \in [1, N] (i \in G_j \text{ or } i \in NG_j \text{ or } i \in NNG_j) \\ \text{and } (\text{dist}(i, k) \leq \tau_2, k \in J)\} \quad (28)$$

where $\text{dist}(i, j)$ denotes the distance between the center point of the group G_j and the center point of the edge i and $\text{dist}(i, k)$ denotes the distance between the center point of groups containing all edges $k \in J$ and the center point of the edge i . τ_1 and τ_2 are two nonzero real values. Generally, the size dimension of the group on the finest level is approximately half of the wavelength (0.5λ). Then the values of τ_1 and τ_2 are recommended to be

$$0.25\lambda \leq \tau_1, \quad \tau_2 \leq 1.0\lambda \quad \text{and} \quad \tau_1 \leq \tau_2$$

It should be noted that the proposed SAI preconditioner operates on all edges in a group at a time, it can reduce the construction cost of the conventional SAI significantly.

4. NUMERICAL EXPERIMENTS

In this section, we show some numerical results for open conducting structures that illustrate the effectiveness of the proposed SAI preconditioner for the solution of the EFIE linear systems in electromagnetic scattering problems. The EFIE linear systems based on the presented hierarchical basis functions of 1.5 order are solved with higher order hierarchical MLFMM accelerated Krylov iterative methods. All numerical experiments are performed on a Pentium 4 with 2.9GHz CPU and 2GB RAM in single precision. The

restarted version of GMRES(m) (generalised minimal residual iterative method) [20] algorithm is used as iterative method, where m is the dimension size of Krylov subspace for GMRES. Additional details and comments on the implementation are given as follows:

- Zero vector is taken as initial approximate solution for all examples and all systems in each example.
- The iteration process is terminated when the normalized backward error is reduced by 10^{-3} for all the examples. The maximum number of iterations is limited to be 600.
- $m = 30$ is used as the dimension of the Krylov subspace for the restarted GMRES method. 1.0 is taken as the relaxation parameter for building the SSOR preconditioner.

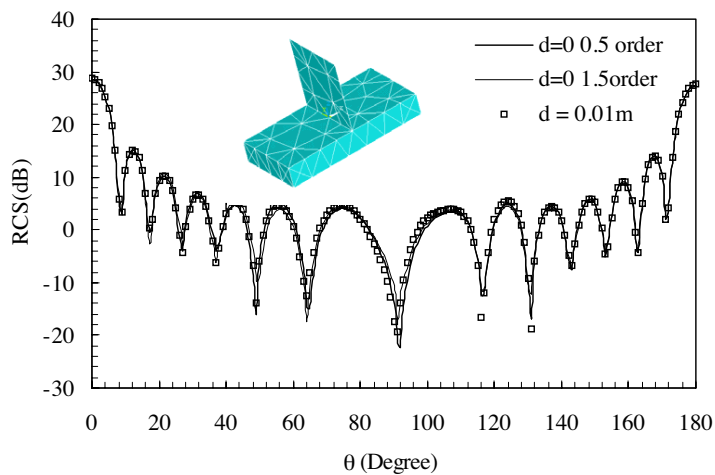


Figure 2. The bistatic RCS for a box-plate scatterer consisting of a plate of size (1 m \times 1 m) placed on an 2 m \times 1 m large plate having a thickness of 0.3 m at 1 GHz.

The first example is a box-plate perfectly electrically conducting (PEC) scatterer consisting of a plate of size (1 m \times 1 m) placed on a 2 m \times 1 m large plate having a thickness of 0.3 m. As shown in Figure 2, the bottom box of the box-plate scatterer has x direction in the longer side and the vertical plate is parallel to y - z plane in the Cartesian coordinate. The operating frequency is 1 GHz. The scatterer is discretized with 12232 curvilinear triangular patches for 0.5 order hierarchical basis functions and 2328 for 1.5 order ones with 18319 and 11614 unknowns, respectively. To verify the accuracy of the method, a closed scatterer consisting of a plate of size (1 m \times 1 m) having a thickness of 0.01 m placed on the above plate is considered.

In our experiments, the restarted version of GMRES (30) algorithm is used. The normalized residual error is taken to be 10^{-3} . The MLFMM algorithm with four levels is employed to speed up the computation of the matrix-vector products involving non-near zone interaction elements. The bi-static RCS of the scatterer with vertical polarization is given in Figure 2 for 0.5 and 1.5 order hierarchical basis functions. The incident angles of plane wave are $\phi^i = 0^\circ$, $\theta^i = 0^\circ$. It can be found that there is an excellent agreement between the box-plate and the closed one. As shown in Table 1, the computation time and memory requirement of the restarted GMRES algorithm is given for the EFIE matrix system with 0.5 and 1.5 order hierarchical basis functions, respectively. It can be seen that the use of the hierarchical higher order basis functions allows the number of unknowns to be reduced by a factor of 1.58.

Table 1. Computation time (in seconds) and memory requirement for a box-plate scatterer.

Basis functions	Unknowns	Iteration step	Solution time	Memory
0.5 order	18319	1193	1951 s	60 MB
1.5 order	11614	9201	9773 s	16 MB

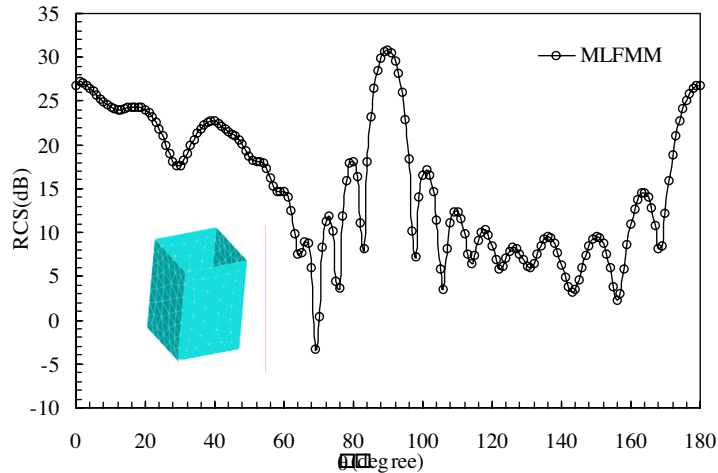


Figure 3. The monostatic RCS for vertical polarization at 300 MHz for an open cavity.

It is also observed that the number of iterations and computation time increases with the order of the hierarchical basis functions because of the increased condition number of the system. In order to accelerate the convergence rate of GMRES algorithm for the EFIE system based on the hierarchical basis functions of order 1.5, the improved SAI preconditioning techniques are developed. We

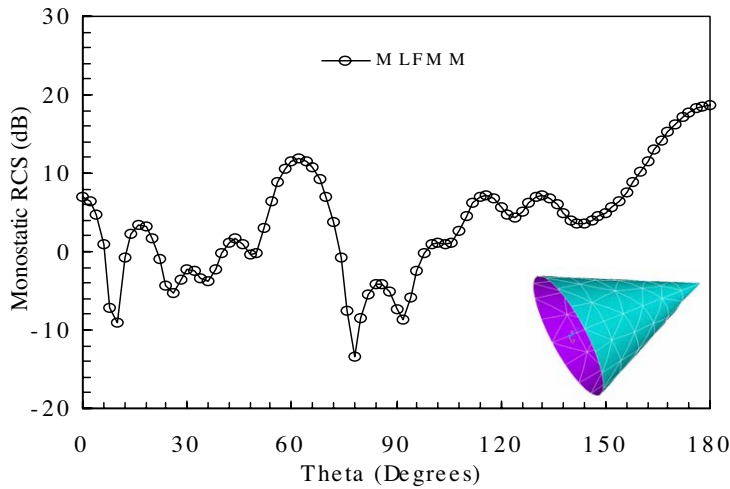


Figure 4. The monostatic RCS for vertical polarization at 3.0 GHz for an open cone.

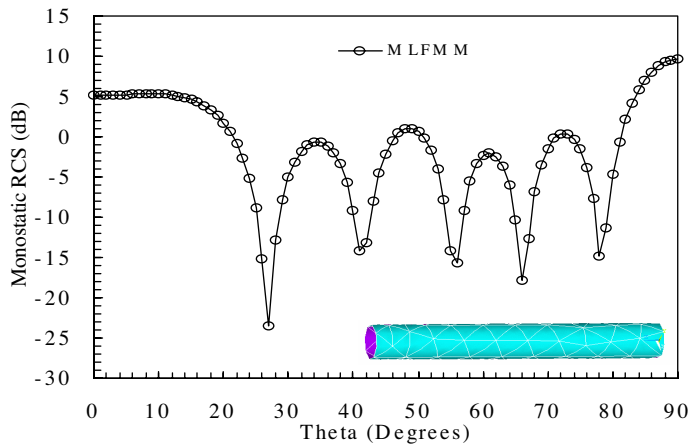


Figure 5. The monostatic RCS for vertical polarization at 300 MHz for an open tube.

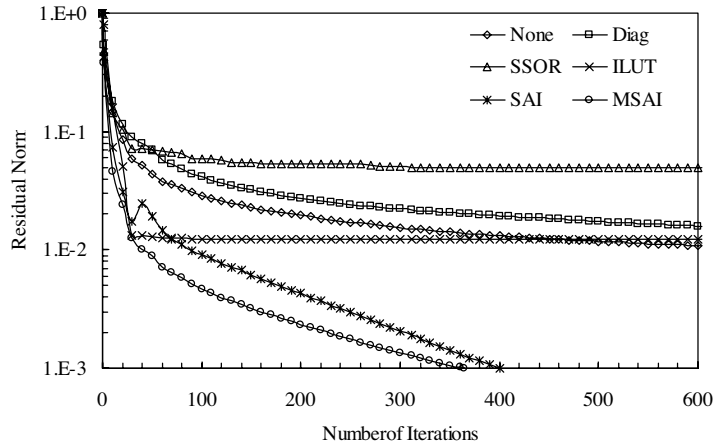


Figure 6. Convergence history of GMRES algorithms on the box-plate example.

investigated the performance of the improved SAI preconditioner on four open conducting structures. The first example is the above box-plate example. The second example is a $2.5\lambda \times 2.5\lambda \times 3.75\lambda$ open cavity with 4698 unknowns for 1.5 order hierarchical basis functions at 300 MHz (λ is wavelength in free space). The third example is a metallic open cone, which has a height of 20 cm and a base whose diameter is also 20 cm. The open cone is discretized with 1632 curvilinear triangular patches for 1.5 order hierarchical basis functions with 8096 unknowns at 3 GHz. The last example is a metallic open circular cylinder (tube), which has a length of 2.76λ and a diameter of 0.432λ . The open tube is discretized with 2412 curvilinear triangular patches for 1.5 order hierarchical basis functions with 12012 unknowns at 300 MHz. The numerical results of monostatic RCS for the other three examples are given in Figures 3–5. It can be found that the result using 1.5 order hierarchical basis agree well with the result in [26–28].

In order to further investigate the performance of the proposed improved SAI preconditioner, the convergence history of GMRES algorithms with different preconditioners for all examples is shown in Figs. 6–9, where Diag denotes the diagonal preconditioner, ILUT denotes the ILU preconditioner dynamically control fill-ins during the construction process [20], SSOR denotes the symmetric successive over-relaxation preconditioner, and MSAI stands for the improved SAI preconditioner suggested in this paper. It can be found that GMRES algorithm with no preconditioner does not reach convergence in 600 iterations for these four open structures. Furthermore, the

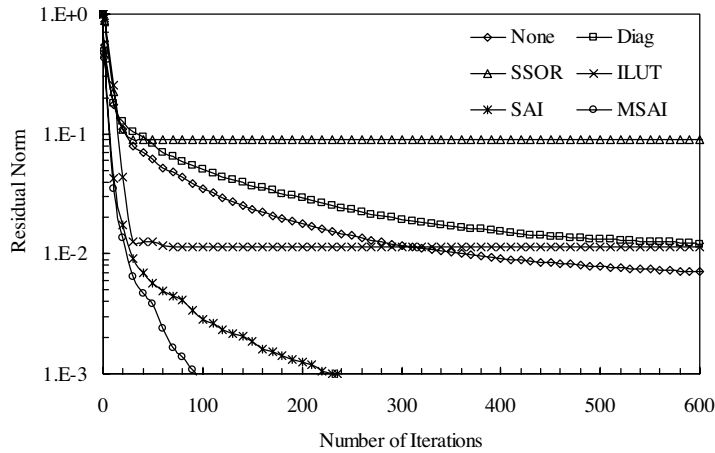


Figure 7. Convergence history of GMRES algorithms on the open cavity example.

diagonal, SSOR and ILUT preconditioned GMRES method slow down the convergence of GMRES algorithm, while both SAI preconditioned GMRES and MSAI preconditioned GMRES reach convergence in less than 600 iterations for all the examples. It can be seen that diagonal, SSOR and ILUT preconditioners deteriorate the convergence of GMRES method on the examples due to the ill-conditioned factors of the preconditioning matrix. It can also be observed that the SAI and MSAI preconditioners are much more efficient than the other preconditioners. When compared with SAI preconditioned GMRES, the improved SAI preconditioned GMRES decreases the number of iterations by a factor of 2.1 on the box-plate example, 2.5 on the open cavity example, 2.6 on the open cone example, and 2.0 on the open tube example. This demonstrates the efficiency of the newly proposed SAI preconditioner for open structures.

Since a good preconditioner depends not only on its effect on convergence but also on its construction and implementation time. The construction time and total solution time of GMRES algorithms with different preconditioners on all examples are given in Tables 2–5, where * refers to no convergence after maximum 600 iterations and the density of a preconditioner is defined by the ratio of the number of non-zero entries in the preconditioning matrix to the number of entries in the full EFIE impedance matrix. It can be found that the MSAI preconditioner reduces the construction cost significantly while maintains good quality compared with the conventional SAI preconditioner. This justifies the use of grouping information from

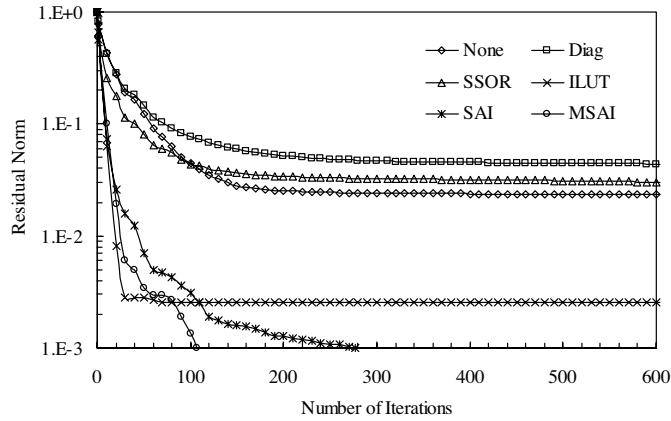


Figure 8. Convergence history of GMRES algorithms on the open cone example.

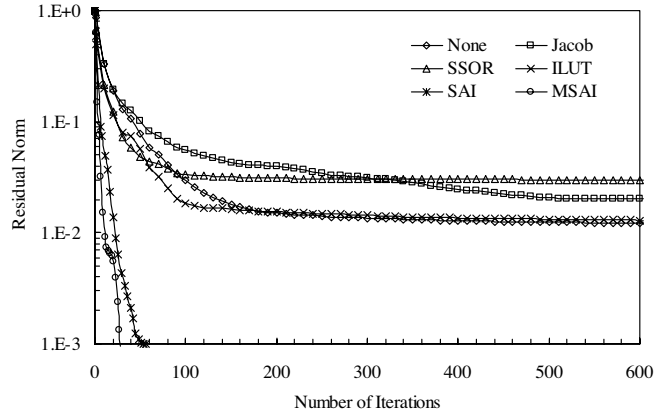


Figure 9. Convergence history of GMRES algorithms on the open tube example.

higher order hierarchical MLFMM for reforming the least-squares problems and for selecting nonzero pattern in the implementation of the MSAI preconditioner. When compared in terms of total solution time (including both the construction time and the iterative solution time), the MSAI preconditioner has a gain over the general SAI preconditioner by a factor of 11.4 on the box-plate example, 20.7 on the open cavity example, 16.2 on the open cone example, and 18.2 on the open tube example.

Table 2. Comparison of the cost and performance of different preconditioners on the box-plate example.

	Density	Construction time	Iterations	Solution time	Total time
SSOR	0.73%	-	*	*	*
ILUT	2.5%	3723 s	*	*	*
SAI	1.39%	4572 s	365	525 s	5097 s
MSAI	2.21%	236 s	176	212 s	448 s

Table 3. Comparison of the cost and performance of different preconditioners on the open cavity example.

	Density	Construction time	Iterations	Solution time	Total time
SSOR	1.89%	-	*	*	*
ILUT	6.28%	1391 s	*	*	*
SAI	1.87%	529 s	235	112 s	641 s
MSAI	1.84%	6 s	94	25 s	31 s

Table 4. Comparison of the cost and performance of different preconditioners on the open cone example.

	Density	Construction time	Iterations	Solution time	Total time
SSOR	1.11%	-	*	*	*
ILUT	3.67%	3059 s	*	*	*
SAI	2.01%	6464 s	277	159 s	6623 s
MSAI	3.76%	332 s	107	78 s	410 s

5. CONCLUSIONS AND COMMENTS

In this paper, a new set of higher order hierarchical basis functions based on curvilinear triangular patch is proposed for EFIE solved using the MLFMM with a reduced computational complexity. Information from higher order hierarchical MLFMM is employed to develop high

Table 5. Comparison of the cost and performance of different preconditioners on the open tube example.

	Density	Construction time	Iterations	Solution time	Total time
SSOR	0.8%	-	*	*	*
ILUT	4.54%	5723 s	*	*	*
SAI	1.465%	14834 s	56	185 s	15019 s
MSAI	2.26%	726 s	28	96 s	822 s

quality of SAI preconditioner when solving large dense linear systems that arise in the EFIE formulation of electromagnetic scattering problems. The key idea is to block several independent least-squares problems into one for all edges in a group. Thus, the N independent least-squares problems in the construction of the general SAI preconditioner are reduced to M (group number) reformed least-squares problems, which save the construction cost significantly. Moreover, two filtration strategies are proposed to capture stronger coupling between higher order hierarchical basis functions for proper nonzero pattern selection. Numerical experiments on several open structure examples are performed and the comparison is made with other preconditioners. It can be found that the proposed SAI preconditioner is more efficient and can significantly reduce the overall computational cost.

ACKNOWLEDGMENT

The authors would like to thank the support of Natural Science Foundation of China under Contract Number 60701005, 60431010, China Postdoctoral Science Foundation under Contract Number 20070411054, Jiangsu Planned Projects for Postdoctoral Research Funds under Contract Number 0701017B and the Research Fund for the Doctoral Program of Higher Education under Contract Number 20070288043.

REFERENCES

1. Su, D., D.-M. Fu, and D. Yu, "Genetic algorithms and method of moments for the design of PIFAs," *Progress In Electromagnetics Research Letters*, Vol. 1, 9–18, 2008.

2. Mittra, R. and K. Du, "Characteristic basis function method for iteration-free solution of large method of moments problems," *Progress In Electromagnetics Research B*, Vol. 6, 307–336, 2008.
3. Huang, E. X. and A. K. Fung, "An application of sampling theorem to moment method simulation in surface scattering," *Journal of Electromagnetic Waves and Applications*, Vol. 20, No. 4, 531–546, 2006.
4. Wang, C.-F. and Y.-B. Gan, "2d cavity modeling using method of moments and iterative solvers," *Progress In Electromagnetics Research*, PIER 43, 123–142, 2003.
5. Danesfahani, R., S. Hatamzadeh-Varmazyar, E. Babolian, and Z. Masouri, "Applying Shannon wavelet basis functions to the method of moments for evaluating the radar cross section of the conducting and resistive surfaces," *Progress In Electromagnetics Research B*, Vol. 8, 257–292, 2008.
6. Varmazyar, S. H. and M. N. Moghadasi, "An integral equation modeling of electromagnetic scattering from the surfaces of arbitrary resistance distribution," *Progress In Electromagnetics Research B*, Vol. 3, 157–172, 2008.
7. Hatamzadeh-Varmazyar, S., M. Naser-Moghadasi, and Z. Masouri, "A moment method simulation of electromagnetic scattering from conducting bodies," *Progress In Electromagnetics Research*, PIER 81, 99–119, 2008.
8. Rao, S. M., D. R. Wilton, and A. W. Glisson, "Electromagnetic scattering by surfaces of arbitrary shape," *IEEE Transactions on Antennas and Propagation*, Vol. 30, No. 3, 409–418, 1982.
9. Chew, W. C., J. M. Jin, E. Midielssen, and J. M. Song, *Fast and Efficient Algorithms in Computational Electromagnetics*, Artech House, Boston, MA, 2001.
10. Fan, Z. H., D. Z. Ding, and R. S. Chen, "The efficient analysis of electromagnetic scattering from composite structures using hybrid CFIE-IEFIE," *Progress In Electromagnetics Research B*, Vol. 10, 131–143, 2008.
11. Pan, X.-M. and X.-Q. Sheng, "A highly efficient parallel approach of multi-level fast multipole algorithm," *Journal of Electromagnetic Waves and Applications*, Vol. 20, No. 8, 1081–1092, 2006.
12. Li, L. and Y.-J. Xie, "Efficient algorithm for analyzing microstrip antennas using fast-multipole algorithm combined with fixed realimage simulated method," *Journal of Electromagnetic Waves and Applications*, Vol. 20, No. 15, 2177–2188, 2006.

13. Wang, P. and Y.-J. Xie, "Scattering and radiation problem of surface/surface junction structure with multilevel fast multipole algorithm," *Journal of Electromagnetic Waves and Applications*, Vol. 20, No. 15, 2189–2200, 2006.
14. Zhao, X. W., C.-H. Liang, and L. Liang, "Multilevel fast multipole algorithm for radiation characteristics of shipborne antennas above seawater," *Progress In Electromagnetics Research*, PIER 81, 291–302, 2008.
15. Zhao, X. W., X.-J. Dang, Y. Zhang, and C.-H. Liang, "The multilevel fast multipole algorithm for EMC analysis of multiple antennas on electrically large platforms," *Progress In Electromagnetics Research*, PIER 69, 161–176, 2007.
16. Andersen, L. S. and J. L. Volakis, "Development and application of a novel class of hierarchical tangential vector finite elements for electromagnetics," *IEEE Transactions on Antennas and Propagation*, Vol. 47, No. 1, 112–120, Jan. 1999.
17. Jorgensen, E., J. L. Volakis, P. Meincke, and O. Breinbjerg, "Higher order hierarchical legendre basis functions for electromagnetic modeling," *IEEE Transactions on Antennas and Propagation*, Vol. 52, No. 11, 2985–2995, Nov. 2004.
18. Chew, W. C., I. T. Chiang, et al., "Integral equation solvers for real world applications — Some challenge problems," *Proceedings of IEEE International Symposium on Antennas and Propagation*, Albuquerque, NM, 91–93, 2006.
19. Song, J. M., C. C. Lu, and W. C. Chew, "Multilevel fast multipole algorithm for electromagnetic scattering by large complex objects," *IEEE Transactions on Antennas and Propagation*, Vol. 45, No. 10, 1488–1493, Oct. 1997.
20. Saad, Y., *Iterative Methods for Sparse Linear Systems*, PWS Publishing Company, 1996.
21. Chow, E. and Y. Saad, "Experimental study of ILU preconditioners for indefinite matrices," *Journal of Computational and Applied Mathematics*, Vol. 86, 387–414, 1997.
22. Rui, P. L., R. S. Chen, Z. H. Fan, J. Hu, and Z. P. Nie, "Perturbed incomplete ILU preconditioner for efficient solution of electric field integral equations," *IET Microwaves, Antennas & Propagation*, Vol. 1, No. 5, 1059–1063, Oct. 2007.
23. Carpentieri, B., I. S. Duff, L. Griud, and G. Alleon, "Combining fast multipole techniques and an approximate inverse preconditioner for large electromagnetism calculations," *SIAM Journal on Scientific Computing*, Vol. 27, No. 3, 774–792, 2005.

24. Rui, P. L. and R. S. Chen, "An efficient sparse approximate inverse preconditioning for FMM implementation," *Microwave and Optical Technology Letters*, Vol. 49, No. 7, 1746–1750, 2007.
25. Graglia, R. D., D. R. Wilton, and A. F. Peterson, "Higher order interpolatory vector bases for computational electromagnetic," *IEEE Transactions on Antennas and Propagation*, Vol. 45, No. 3, 329–342, 1997.
26. Donepudi, K. C., J. M. Jin, J. M. Song, and W. C. Chew, "A higher order parallelized multilevel fast multipole algorithm for 3-D scattering," *IEEE Transactions on Antennas and Propagation*, Vol. 49, No. 7, 1069–1078, 2001.
27. Lee, J.-F., R. Lee, and R. J. Burkholder, "Loop star basis functions and a robust preconditioner for EFIE scattering problems," *IEEE Transactions on Antennas and Propagation*, Vol. 51, 1855–1863, Aug. 2003.
28. Medgyesi-Mitschang, L. N. and J. M. Putnam, "Scattering from finite bodies of translation: Plates, curved surfaces, and noncircular cylinders," *IEEE Transactions on Antennas and Propagation*, Vol. 31, No. 6, 847–852, Nov. 1983.